

Supplementary Figure S3

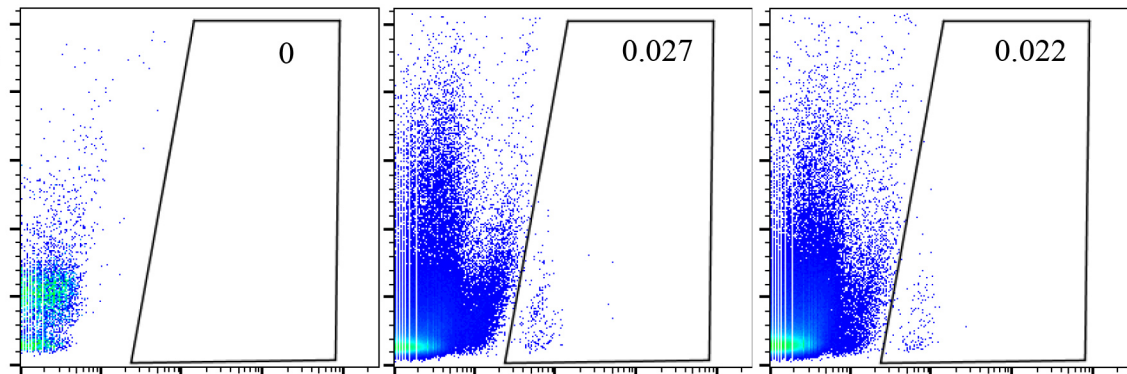
Naïve

treated

PBS

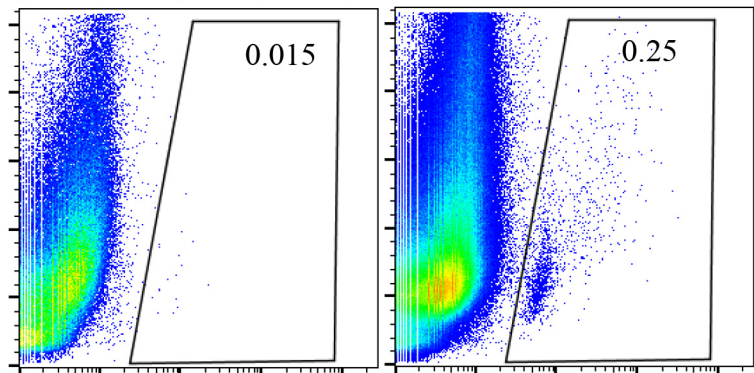
rMVTT

Spleen

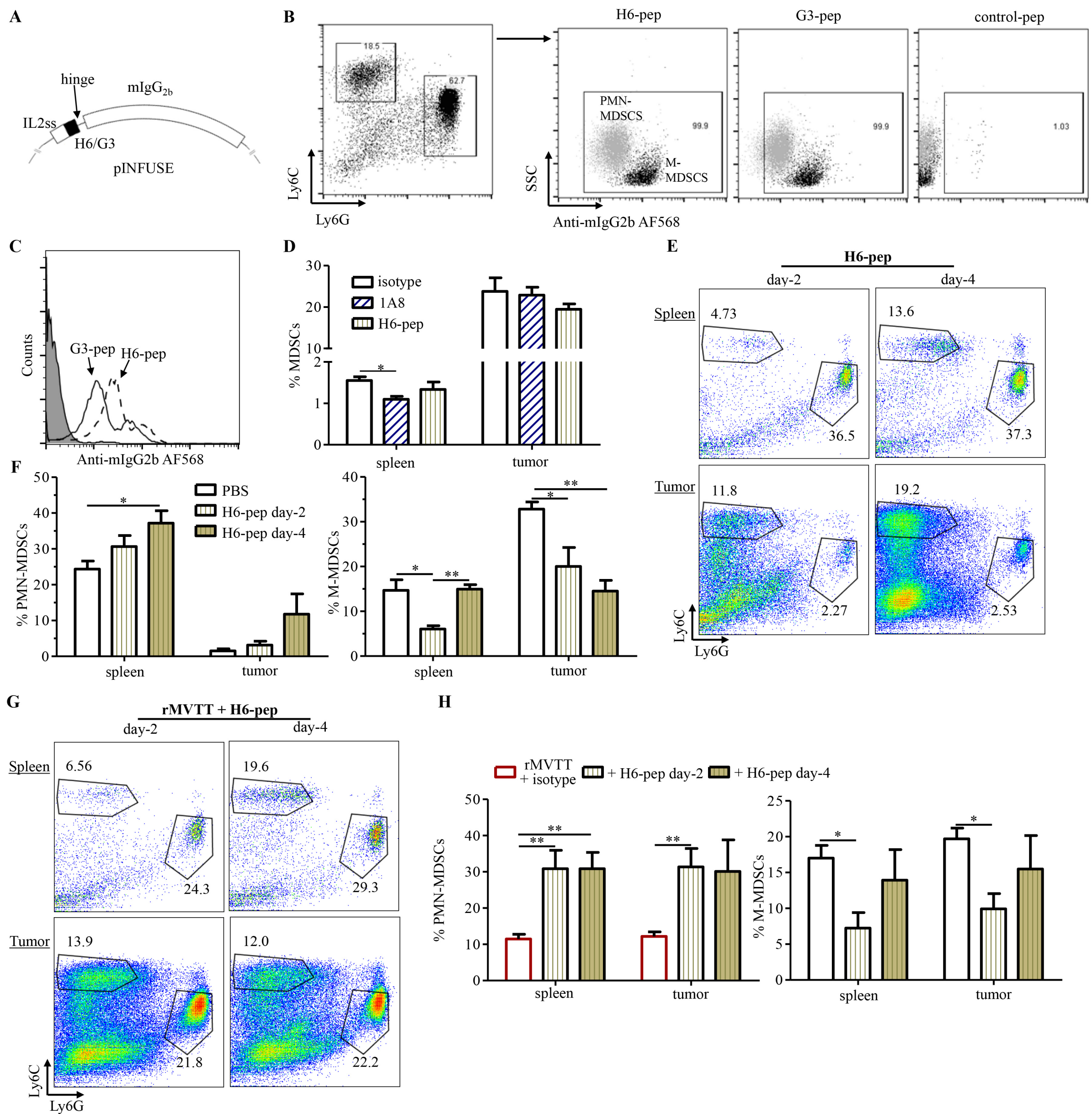


Tumor

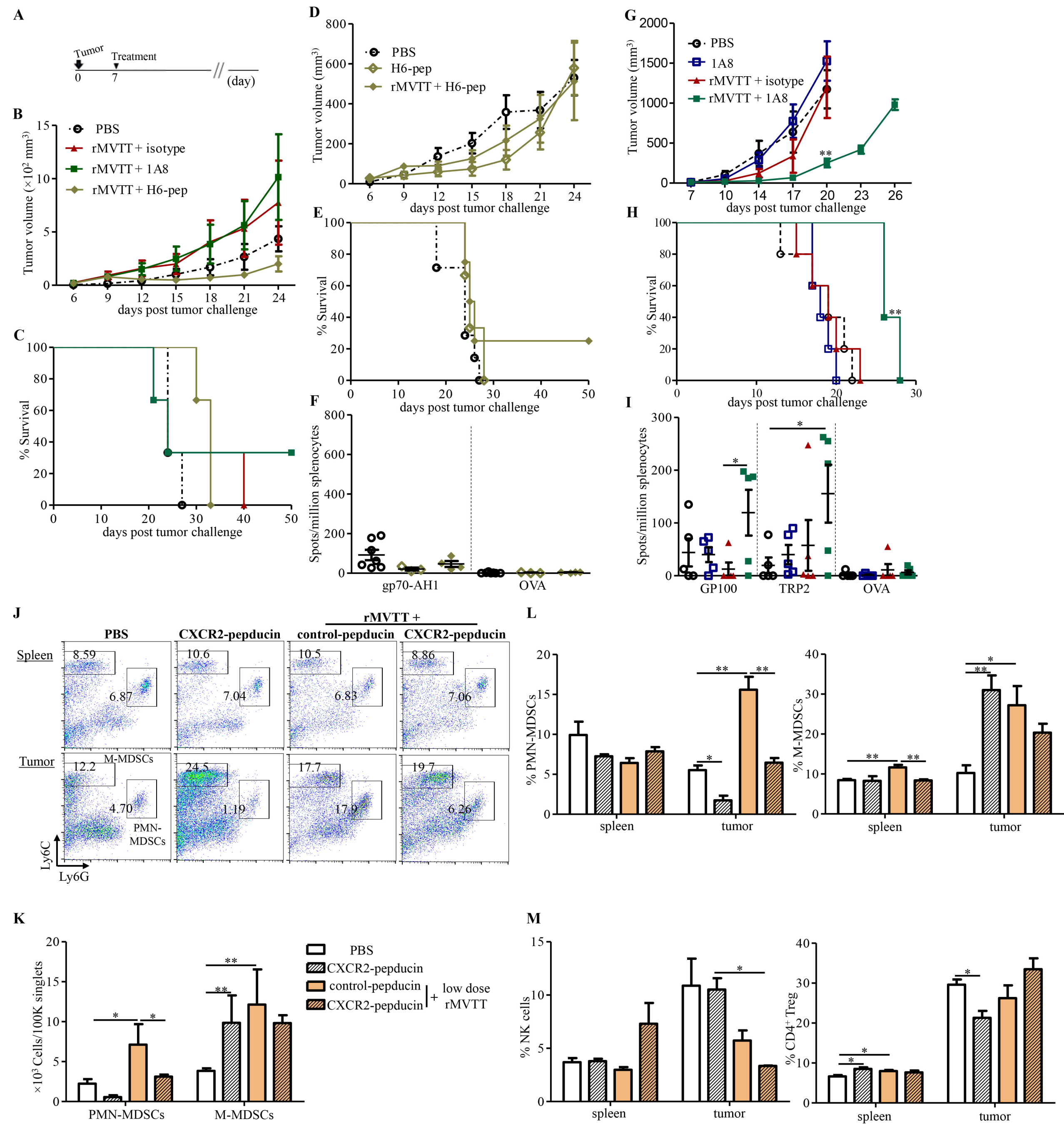
SSC
↑
CFSE
→



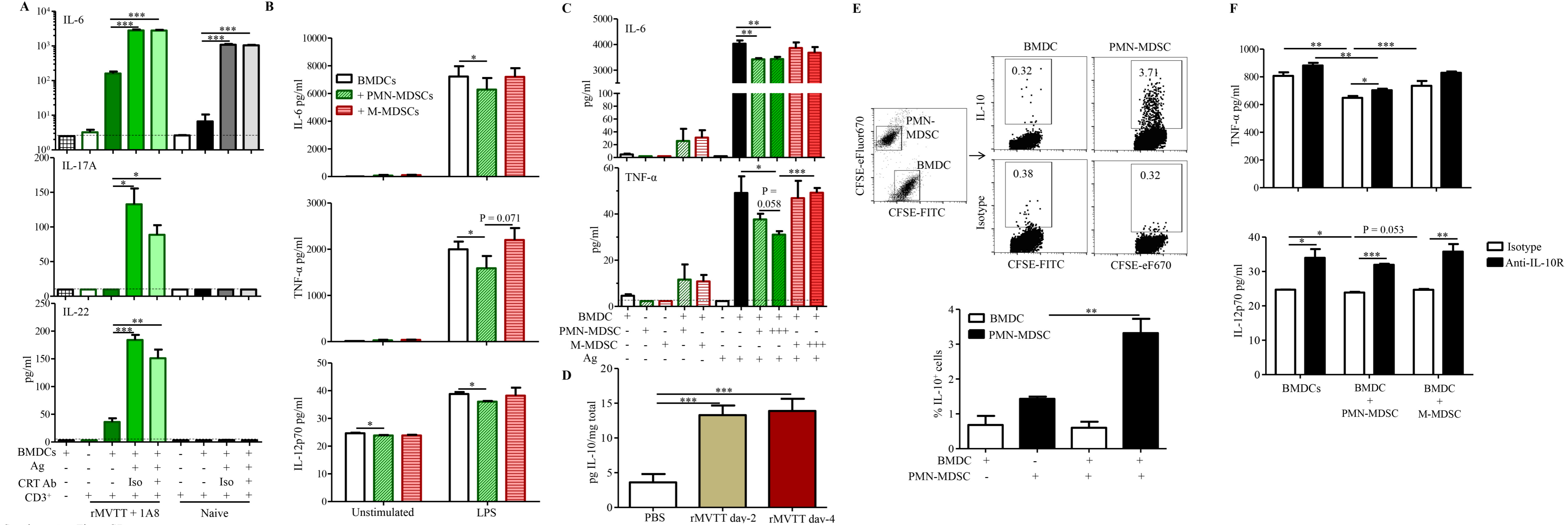
Supplementary Figure S4



Supplementary Figure S5



Supplementary Figure S6



Supplementary Figure S7

Supplementary Figure Legends

Supplementary Figure S1. Generation of rMVTT encoding two detection markers, HIV-1

p24 and HcRed. (A) Schematic representation of the vaccinia shuttle vector pZCxz encoding both HIV-1 p24 and HcRed. Expression of each protein is driven by different promoters. (B) AB1 cells were infected with rMVTT for 24 hours. HcRed signals were acquired with fluorescent microscopy. BF, Bright Field. (C) Western blot analysis of viral protein expression in AB1 cells after rMVTT infection. The anti-p24 antibody (clone: 183-H12-5C) was used to detect the presence of the p24 protein (arrow). GAPDH served as the internal control. (D) AB1 cells were seeded in 24-well plates at a density of 2×10^5 cells/well. Twenty-four hours later, cells were infected with 0.2 MOI rMVTT virus. Cells were harvested at the three indicated time points, and the percentages of HcRed⁺ AB1 cells were analyzed using flow cytometry. (E) Culture supernatant after rMVTT infection was collected from AB1 cells at different time points, and viral particles in the supernatant were measured. Ctrl, culture medium alone. Data shown are representative of two independent experiments.

Supplementary Figure S2. High-dose MVTT cleared AB1 mesothelioma in SCID mice. $5 \times$

10^5 luciferase-expressing AB1 (AB1-Luc) cells were inoculated s.c into SCID mice 5 days before they received i.t treatment of either MVTT or PBS. MVTT-treated mice (n = 3) received 1×10^8 PFU rMVTT per dose every 2 days for 5 injections. Tumor growth was measured by either bioluminescent signals (A) with representative bioluminescence images (B) or tumor volumes (C).

Supplementary Figure S3. MVTT treatment recruited PMN-MDSCs into the TME. (A)

Expression of HcRed in established AB1 mesothelioma tumors after rMVTT treatment. Overlay of representative light and fluorescent images of HcRed in the tumor with or without rMVTT injection (*left panel*). Fluorescence images were acquired using an IVIS Spectrum instrument. The color bar indicates the fluorescence radiant efficiency multiplied by 10^7 . Representative images are shown. HcRed fluorescent signals from tumors were calculated (*right panel*). **(B)** Immunohistochemistry of vaccinia virus proteins in AB1 tumors 2 days post rMVTT injection. AB1 tumor sections were stained with hematoxylin & eosin (H&E) (*left panel*) or stained for vaccinia virus proteins (Green) using a commercially obtained rabbit anti-vaccinia virus antibody (WR, Access Biomedical) and Hoechst 33258 staining (blue) (*right panel*). Representative images are shown. Dotted line, boundary between infected and un-infected tumor tissue. **(C)** Gating strategies for flow cytometric scatter plots showing identification of MDSC subsets, NK cells, and $CD4^+$ Tregs, as well as $PD1^+/Tim3^+ CD3^+$ T cells. **(D)** Frequencies (*left panel*) and absolute numbers (*right panel*) of $CD3^+$ T cells in the tumor. **(E)** Frequencies of $PD1^+CD3^+$ T cells (*left panel*) and $Tim3^+ CD3^+$ T cells (*right panel*) in the spleen and tumor.

Supplementary Figure S4. Flow cytometric analysis of CFSE-labelled MDSCs. Adoptively

transferred MDSCs accumulated at the tumor site 24 hours after rMVTT treatment in representative mice. Numbers within dot plots represent $CFSE^+$ cell proportions relative to total singlets.

Supplementary Figure S5. Preferential depletion of MDSC subsets by antibody and peptibody treatment. (A) Schematic representation of H6/G3-pep-encoding plasmid. IL2_{ss}, IL2 secretory signal. The binding affinity of H6-pep, G3-pep or peptibody without the 12-mer-specific sequence (control-pep) was measured by flow cytometry. Splenocytes from AB1-tumor bearing mice were incubated with 2 μg of peptibody following detection with anti-mouse IgG_{2b} AF568. (B) Representative dot plots gated on CD11b⁺ cells are shown with numbers indicating cell proportions. (C) Representative histogram plots gated on CD11b⁺ cells are shown with pep-H6 (dashed line), G3-pep (solid line) or control-pep (shaded histogram) staining. (D) Percentages of total MDSCs in the spleen and tumor after i.t administration of 100 μg of 1A8, H6-pep or 2A3 isotype control. Changes in PMN-MDSC and M-MDSC frequencies after i.t H6-pep treatment were shown with representative dot plots (E) and were analyzed (F). After i.t co-administration of 1×10^7 PFU rMVTT and 100 μg of H6-pep, changes in the PMN-MDSC and M-MDSC frequencies are shown (G) and were analyzed (H).

Supplementary Figure S6. Depletion of PMN-MDSCs enhances MVTT treatment efficacy by inducing antitumor T cell immunity. (A) Schematic representation of the treatment schedule where one administration of either PBS, 1A8 only, combined rMVTT and 1A8 or combined rMVTT and H6-pep was given 7 days after AB1 cell inoculation. Tumor growth (B) and survival curve (C) of mice receiving one round of treatment. Tumor growth (D), survival curve (E) and T cell responses of splenocytes (F) in mice receiving 2 injections of PBS, H6-pep or combined rMVTT and H6-pep. C57BL/6 mice were implanted s.c with 5×10^5 B16F10-Luc cells 7 days before treatment. rMVTT, 1A8 antibody, combined rMVTT and 1A8 or PBS control were i.t administered at day 7 and day 9. Tumor growth (G), survival curve (H) and T cell

responses of splenocytes **(I)** at their endpoints were shown. BALB/c mice bearing 6-day AB1 tumors were treated with 2.5 mg/kg control-pepducin or CXCR2-pepducin, followed by 1 mg/kg pepducin daily for the duration of the study. rMVTT were given i.t at day 7 and samples were collected at day 9. **(J)** Representative dot plots showing populations of PMN-MDSCs and M-MDSCs within CD11b⁺ cells in the spleen and tumor. Numbers indicate cell proportions. Absolute cell number **(K)** or percentage **(L)** of PMN-MDSCs and M-MDSCs, and **(M)** Percentage of NK cells and CD4⁺Treg were calculated.

Supplementary Figure S7. PMN-MDSCs prevent the induction of antitumor T cell immunity by restricting DC activation. **(A)** Secretion of IL-6, IL-17A and IL-22 in co-cultures of CD3⁺ T cells and antigen-pulsed BMDCs. Naïve, purified CD3⁺ T cells from naïve BALB/c mice. **(B)** Secreted cytokines in the co-culture supernatant collected 48 hours post incubation. **(C)** Secretion of IL-6 and TNF- α in antigen-pulsed BMDC cultures in the presence of either PMN-MDSCs or M-MDSCs at MDSC:BMDC ratios of 1:1 and 3:1. BMDCs were pulsed with rMVTT-treated AB1 cell supernatants. Data shown are representative of two independent experiments. **(D)** IL-10 production in tumor homogenates after rMVTT treatment. **(E)** Intracellular staining for IL-10 after co-culture of BMDCs and MDSCs. BMDCs and MDSCs were labelled with CFSE-FITC or CFSE-eFluor670, respectively. **(F)** Production of TNF- α and IL-12p70 in the culture supernatant in the presence of IL-10 receptor blocking antibody or isotype control. Culture supernatant were collected 48 hours post incubation and measured for cytokine secretion.